

UDC 539.3

ANALYSIS OF THE STRESS-STRAIN STATE OF A LAYER WITH A CYLINDRICAL CAVITY AND EMBEDDED SUPPORTS WITH BUSHINGS

Mykhailo L. Kosenko

Scs2012kh@gmail.com

ORCID: 0009-0002-2005-2222

National Aerospace University
"Kharkiv Aviation Institute",
17, Vadyma Manka str., Kharkiv,
61070, Ukraine

Using cylindrical embedded supports for parts is common in the aerospace and mechanical engineering industries. Simplifications or approximations are used to calculate such connections. A method for calculating a layer on two longitudinally embedded cylindrical supports is proposed in this paper. There are bushings (thick-walled pipes) between the supports and the layer; the layer is weakened by a longitudinal cylindrical cavity. Stresses are set on the lower and upper surfaces of the layer, smooth contact conditions are set on the inner surfaces of the pipes, and stresses are set on the surface of the cavity. To solve the problem, the Lamé equation is used, where the Cartesian coordinate system is used for the layer, and local cylindrical systems are used for the pipes and the cylindrical cavity. The combination of basic solutions in different coordinate systems is performed using the generalized Fourier method. Based on the boundary conditions and conjugation conditions, an infinite system of integro-algebraic equations, which is reduced to linear algebraic equations of the second kind and solved using the reduction method, is obtained. The stress-strain state at each point of elastic connected bodies is also determined from the Lamé equation using the generalized Fourier method to the basis solutions. The accuracy of the results in this case depends on the approximation of the boundary surfaces to each other and on the order of the system of equations. Numerical studies have been carried out for a layer with supports and a cavity located in a straight line under the action of a cantilever load. The analysis of the stress state was obtained in the zones of cylindrical holes of the layer and in the body of the bushings. The maximum stresses exceed the specified ones and occur at the location of the cylindrical cavity. The proposed solution method makes it possible to obtain the results of the stress-strain state of cantilevered elements of aircraft structures, to evaluate the influence of material and geometric parameters on the values of stress distribution in other structures of machines and mechanisms that can be represented as models similar to the one under consideration.

Keywords: generalized Fourier method, Lamé equation, layer with cylindrical inclusions, infinite system of integro-algebraic equations, cylindrical cavity.

Introduction

In mechanical and aircraft engineering, the combination of various structural elements is often hinged. These elements are connected by bolts, rivets, bearings and other fasteners, for which the corresponding holes are provided in the structures. Thus, elements in which the supports are embedded cylinders are created. To strengthen the contact point with the support, bushings, rigidly connected to the part and smoothly contacting the support, are often installed in the parts.

For the calculation of such nodes, which are a layer with thick-walled pipes, approximate methods, such as the finite element method [1], and software tools based on it [2], are mainly used. However, with this approach, to confirm the obtained results, it is worth using analytical or analytical-numerical methods, or conducting tests [3, 4].

The use of analytical methods [5, 6] based on the expansion of solutions into a Fourier series is possible only with a significant simplification of the calculation model. The specified methods consider the problem either in a flat form or with the number of boundary conditions less than three.

Analytical-numerical methods, in comparison with analytical ones, provide more opportunities for estimating the stress state of a layer with cylindrical inhomogeneities. Thus, in papers [7, 8] a layer with a cylindrical cavity located perpendicular to the boundaries of the layer is considered. The solution is based on the integral Laplace transforms and finite Fourier sine and cosine series, which are sequentially applied to the axisymmetric equations of motion and boundary conditions. However, in the case of using the proposed method [7, 8], no more than one cylindrical cavity can be taken into account.

This work is licensed under a Creative Commons Attribution 4.0 International License.

© Mykhailo L. Kosenko, 2025

In paper [9], thanks to the integral Weber-Orr transforms, the problem of torsion of an elastic half-space with a vertical cylindrical cavity is studied, while a coaxial stamp rotating under the action of a torque is fixed on the flat boundary. The method proposed in this study can only be used for half-space.

To achieve the optimal distribution of thermal stresses in composite plates with non-circular holes under uniform heat flux, metaheuristic optimization algorithms are used in [10]. The analytical part of the study is based on thermoelastic theory and the complex variable method. However, the proposed method [10] cannot take into account more than one cylindrical cavity.

To calculate a layer with several cylindrical inhomogeneities located parallel to the layer boundaries, an approach based on the analytical-numerical generalized Fourier method [11], which allows combining the basic solutions of the Lamé equation in different coordinate systems, is useful. Thus, using the generalized Fourier method, problems for a cylinder with cylindrical cavities [12, 13] and inclusions [14] were solved. In [15], using the example of a problem for a half-space with a cylindrical cavity, the justification of the formulas for the transition of basic solutions between the Cartesian and cylindrical coordinate systems is given. Based on the generalized Fourier method, in [16], the problem for a layer with one longitudinal cylindrical cavity was solved, and in paper [17] – the problem for a layer with a continuous cylindrical inclusion was solved. The problem for a layer connected to a half-space in which a cylindrical cavity is located is solved in [18]. A layer with two cylindrical cavities (simulated embedded cylindrical supports) is considered in [19]. The problem for a layer with one thick-walled pipe is solved in [20], for a layer with one thick-walled pipe and a cylindrical cavity – in [21], with two thick-walled pipes (simulated cylindrical embedded supports with bushings) – in [22]. However, the approaches proposed in [16–22] cannot be applied to the solution of the problem for a layer on two cylindrical embedded supports with bushings, weakened by a cylindrical cavity.

The aim of this paper is:

– to develop a method for solving a mixed problem of the theory of elasticity for a layer with two longitudinal cylindrical pipes and a cylindrical cavity. To achieve this, stresses are given on the upper and lower boundaries of the layer, smooth contact conditions are imposed on the inner surfaces of the pipes, and stresses are imposed on the cavity;

– to analyze the stress state of the layer and thick-walled pipes under a given cantilever load.

Problem statement

The model is a layer with two cylindrical thick-walled pipes and a cylindrical cavity located parallel to its boundaries (Fig. 1).

Local cylindrical coordinates are used to describe the geometry of the pipes and cavity (ρ_p, φ_p, z , where p – pipe or cavity number), and Cartesian coordinate system (x, y, z) , which coincides with the coordinate system of the first pipe ($p=1$), is used for the layer.

The outer radii of the pipes or cavity are denoted as R_p , and the inner radii of the pipes – as r_p . Distance to layer boundaries is $y=h$ and $y=-\tilde{h}$.

To solve the problem, we look for a solution to the Lamé equations $\Delta \vec{u} + (1-2\sigma)^{-1} \nabla \operatorname{div} \vec{u} = 0$, under given boundary conditions:

– at the upper and lower boundaries of the layer, the stresses are set as

$$\bar{F}\vec{U}(x, z)|_{y=h} = \bar{F}_h^0(x, z); \quad \bar{F}\vec{U}(x, z)|_{y=-\tilde{h}} = \bar{F}_{\tilde{h}}^0(x, z)$$

where

$$\bar{F}_h^0(x, z) = \tau_{yx}^{(h)} \cdot \vec{e}_x + \sigma_y^{(h)} \cdot \vec{e}_y + \tau_{yz}^{(h)} \cdot \vec{e}_z; \quad \bar{F}_{\tilde{h}}^0(x, z) = \tau_{yx}^{(\tilde{h})} \cdot \vec{e}_x + \sigma_y^{(\tilde{h})} \cdot \vec{e}_y + \tau_{yz}^{(\tilde{h})} \cdot \vec{e}_z; \quad (1)$$

– smooth contact conditions are specified on the inner surfaces of the pipes

$$\left. \begin{array}{l} U_p(\varphi_p, z) \Big|_{\rho_p=R_p} = U_0^{(p)}(\varphi_p, z) \\ \tau_{\rho\varphi} \Big|_{\rho_p=R_p} = \tau_1^{(p)}(\varphi_p, z) \\ \tau_{\rho z} \Big|_{\rho_p=R_p} = \tau_2^{(p)}(\varphi_p, z) \end{array} \right\} \quad (2)$$

– on the surface of a cylindrical cavity ($p = 3$), the stresses are set as

$$F\vec{U}(\varphi_3, z) \Big|_{\rho_3=R_3} = \vec{F}_3^0(\varphi_3, z) = \sigma_{\rho}^{(3)}\vec{e}_{\rho} + \tau_{\rho\varphi}^{(3)}\vec{e}_{\varphi} + \tau_{\rho z}^{(3)}\vec{e}_z, \quad (3)$$

where \vec{U} is the displacement in a layer; $F\vec{U} = 2G \left[\frac{\sigma}{1-2\sigma} \vec{n} \cdot \overline{\operatorname{div} U} + \frac{\partial}{\partial n} \vec{U} + \frac{1}{2} (\vec{n} \times \overline{\operatorname{rot} U}) \right]$ is the stress operator.

The layer is rigidly connected to each pipe by the conjugation conditions

$$\vec{U}_0(\varphi, z) \Big|_{\rho=R_p} = \vec{U}_p(\varphi, z) \Big|_{\rho=R_p}; \quad (4)$$

$$F\vec{U}_0(\varphi, z) \Big|_{\rho=R_p} = F\vec{U}_p(\varphi, z) \Big|_{\rho=R_p}, \quad (5)$$

where $\vec{U}_0(\varphi, z)$ is the solution for the layer; $\vec{U}_p(\varphi, z)$ is the solution for pipes.

All given functions will be considered to be rapidly decreasing from the origin along the axis z and along the axis x .

Solution methodology

The solution to the problem is given in the form proposed in [22], taking into account the additional cavity

$$\begin{aligned} \vec{U}_0 &= \sum_{p=1}^3 \sum_{k=1}^3 \int_{-\infty}^{\infty} \sum_{m=-\infty}^{\infty} B_{k,m}^{(p)}(\lambda) \cdot \vec{S}_{k,m}(\rho_p, \varphi_p, z; \lambda) d\lambda + \\ &+ \sum_{k=1}^3 \int_{-\infty}^{\infty} \int_{-\infty}^{\infty} (H_k(\lambda, \mu) \cdot \vec{u}_k^{(+)}(x, y, z; \lambda, \mu) + \tilde{H}_k(\lambda, \mu) \cdot \vec{u}_k^{(-)}(x, y, z; \lambda, \mu)) d\mu d\lambda; \end{aligned} \quad (6)$$

$$\begin{aligned} \vec{U}_1 &= \sum_{k=1}^3 \int_{-\infty}^{\infty} \sum_{m=-\infty}^{\infty} A_{k,m}^{(1)}(\lambda) \cdot \vec{R}_{k,m}(\rho_1, \varphi_1, z; \lambda) + \tilde{A}_{k,m}^{(1)}(\lambda) \cdot \vec{S}_{k,m}(\rho_1, \varphi_1, z; \lambda) d\lambda; \\ \vec{U}_2 &= \sum_{k=1}^3 \int_{-\infty}^{\infty} \sum_{m=-\infty}^{\infty} A_{k,m}^{(2)}(\lambda) \cdot \vec{R}_{k,m}(\rho_2, \varphi_2, z; \lambda) + \tilde{A}_{k,m}^{(2)}(\lambda) \cdot \vec{S}_{k,m}(\rho_2, \varphi_2, z; \lambda) d\lambda, \end{aligned} \quad (7)$$

where $H_k(\lambda, \mu)$, $\tilde{H}_k(\lambda, \mu)$, $B_{k,m}^{(p)}(\lambda)$, $A_{k,m}^{(1)}(\lambda)$, $\tilde{A}_{k,m}^{(1)}(\lambda)$, $A_{k,m}^{(2)}(\lambda)$, $\tilde{A}_{k,m}^{(2)}(\lambda)$ are 27 unknown functions ($k=1..3$, $p=1..3$), which must be found from the boundary conditions (1)–(3) and the conjugation conditions (4), (5); $\vec{S}_{k,m}(\rho_p, \varphi_p, z; \lambda)$, $\vec{R}_{k,m}(\rho_p, \varphi_p, z; \lambda)$, $\vec{u}_k^{(+)}(x, y, z; \lambda, \mu)$, $\vec{u}_k^{(-)}(x, y, z; \lambda, \mu)$ are basic solutions of the Lamé equation, given in the form [11]

$$\begin{aligned} \vec{u}_k^{\pm}(x, y, z; \lambda, \mu) &= N_k^{(d)} e^{i(\lambda z + \mu x) \pm \gamma y}; \\ \vec{R}_{k,m}(\rho, \varphi, z; \lambda) &= N_k^{(p)} I_m(\lambda \rho) e^{i(\lambda z + m\varphi)}; \quad \vec{S}_{k,m}(\rho, \varphi, z; \lambda) = N_k^{(p)} [(sign \lambda)^m K_m(|\lambda| \rho) \cdot e^{i(\lambda z + m\varphi)}]; \quad k=1, 2, 3; \\ N_1^{(d)} &= \frac{1}{\lambda} \nabla; \quad N_2^{(d)} = \frac{4}{\lambda} (v-1) \vec{e}_2^{(1)} + \frac{1}{\lambda} \nabla (y \cdot); \quad N_3^{(d)} = \frac{i}{\lambda} \operatorname{rot}(\vec{e}_3^{(1)} \cdot); \\ N_1^{(p)} &= \frac{1}{\lambda} \nabla; \quad N_2^{(p)} = \frac{1}{\lambda} \left[\nabla \left(\rho \frac{\partial}{\partial \rho} \right) + 4(v-1) \left(\nabla - \vec{e}_3^{(2)} \frac{\partial}{\partial z} \right) \right]; \quad N_3^{(p)} = \frac{i}{\lambda} \operatorname{rot}(\vec{e}_3^{(2)} \cdot); \quad \gamma = \sqrt{\lambda^2 + \mu^2}; \\ &- \infty < \lambda, \mu < \infty, \end{aligned}$$

where v is the Poisson's; $I_m(x)$, $K_m(x)$ are modified Bessel functions.

To write equations (6) and (7) in the same coordinate system, the transition formulas between the basic solutions of the Lamé equation were applied [11]:

– from external solutions for the cylinder $\vec{S}_{k,m}$ to solutions for the layer $\vec{u}_k^{(-)}$ (at $y>0$) and $\vec{u}_k^{(+)}$ (at $y<0$)

$$\vec{S}_{k,m}(\rho_p, \varphi_p, z; \lambda) = \frac{(-i)^m}{2} \int_{-\infty}^{\infty} \omega_{\mp}^m \cdot e^{-i\mu\bar{x}_p \pm \bar{\gamma}_p} \cdot \vec{u}_k^{(\mp)} \cdot \frac{d\mu}{\gamma}, \quad k=1, 3;$$

$$\vec{S}_{2,m}(\rho_p, \varphi_p, z; \lambda) = \frac{(-i)^m}{2} \int_{-\infty}^{\infty} \omega_{\mp}^m \cdot \left(\left(\pm m \cdot \mu - \frac{\lambda^2}{\gamma} \pm \lambda^2 \bar{y}_p \right) \vec{u}_1^{(\mp)} \mp \lambda^2 \vec{u}_2^{(\mp)} \pm 4\mu(1-\sigma) \vec{u}_3^{(\mp)} \right) \cdot \frac{e^{-i\mu\bar{x}_p \pm \gamma\bar{y}_p} d\mu}{\gamma^2} \quad (8)$$

where $\gamma = \sqrt{\lambda^2 + \mu^2}$, $\omega_{\mp}(\lambda, \mu) = \frac{\mu \mp \gamma}{\lambda}$, $m = 0, \pm 1, \pm 2, \dots$;

– from the solutions of the layer $\vec{u}_k^{(+)}$ and $\vec{u}_k^{(-)}$ to the internal solutions of the cylinder $\vec{R}_{k,m}$

$$\vec{u}_k^{(\pm)}(x, y, z) = e^{i\mu\bar{x}_p \pm \gamma\bar{y}_p} \cdot \sum_{m=-\infty}^{\infty} (i \cdot \omega_{\mp})^m \vec{R}_{k,m}, \quad k=1, 3;$$

$$\vec{u}_2^{(\pm)}(x, y, z) = e^{i\mu\bar{x}_p \pm \gamma\bar{y}_p} \cdot \sum_{m=-\infty}^{\infty} [(i \cdot \omega_{\mp})^m \cdot \lambda^{-2} ((m \cdot \mu + \bar{y}_p \cdot \lambda^2) \cdot \vec{R}_{1,m} \pm \gamma \cdot \vec{R}_{2,m} + 4\mu(1-\sigma) \vec{R}_{3,m})], \quad (8)$$

where $\vec{R}_{k,m} = \tilde{b}_{k,m}(\rho_p, \lambda) \cdot e^{i(m\varphi_p + \lambda z)}$; $\tilde{b}_{1,n}(\rho, \lambda) = \vec{e}_\rho \cdot I'_n(\lambda\rho) + i \cdot I_n(\lambda\rho) \cdot \left(\vec{e}_\varphi \frac{n}{\lambda\rho} + \vec{e}_z \right)$;

$$\tilde{b}_{2,n}(\rho, \lambda) = \vec{e}_\rho \cdot [(4\sigma - 3) \cdot I'_n(\lambda\rho) + \lambda\rho I''_n(\lambda\rho)] + \vec{e}_\varphi i \cdot m \left(I'_n(\lambda\rho) + \frac{4(\sigma-1)}{\lambda\rho} I_n(\lambda\rho) \right) + \vec{e}_z i \lambda\rho I'_n(\lambda\rho);$$

$$\tilde{b}_{3,n}(\rho, \lambda) = - \left[\vec{e}_\rho \cdot I_n(\lambda\rho) \frac{n}{\lambda\rho} + \vec{e}_\varphi \cdot i \cdot I'_n(\lambda\rho) \right]; \quad \vec{e}_\rho, \vec{e}_\varphi, \vec{e}_z \text{ are orts in a cylindrical coordinate system};$$

– from solutions of the cylinder with number p to solutions of the cylinder with number q

$$\begin{aligned} \vec{S}_{k,m}(\rho_p, \varphi_p, z; \lambda) &= \sum_{n=-\infty}^{\infty} \vec{b}_{k,pq}^{mn}(\rho_q) \cdot e^{i(n\varphi_q + \lambda z)}, \quad k=1, 2, 3; \\ \vec{b}_{1,pq}^{mn}(\rho_q) &= (-1)^n \tilde{K}_{m-n}(\lambda \ell_{pq}) \cdot e^{i(m-n)\alpha_{pq}} \cdot \tilde{b}_{1,n}(\rho_q, \lambda); \quad \vec{b}_{3,pq}^{mn}(\rho_q) = (-1)^n \tilde{K}_{m-n}(\lambda \ell_{pq}) \cdot e^{i(m-n)\alpha_{pq}} \cdot \tilde{b}_{3,n}(\rho_q, \lambda); \\ \vec{b}_{2,pq}^{mn}(\rho_q) &= (-1)^n \left\{ \tilde{K}_{m-n}(\lambda \ell_{pq}) \cdot \tilde{b}_{2,n}(\rho_q, \lambda) - \frac{\lambda}{2} \ell_{pq} \cdot [\tilde{K}_{m-n+1}(\lambda \ell_{pq}) + \tilde{K}_{m-n-1}(\lambda \ell_{pq})] \cdot \tilde{b}_{1,n}(\rho_q, \lambda) \right\} \cdot e^{i(m-n)\alpha_{pq}}, \quad (9) \end{aligned}$$

where α_{pq} is the angle between the axis x_p and a segment ℓ_{qp} ; $\tilde{K}_m(x) = (\text{sign}(x))^m \cdot K_m(|x|)$.

To find the 27 unknown functions (6) and (7), a system of 27 integro-algebraic equations was formed.

The first six equations are formed when the boundary conditions on the flat surfaces of the layer (1) are satisfied. For this, the stress operator is applied to the functions (6), and the double Fourier integral – to (1), after which they are equated to each other. Basic solutions $\vec{S}_{k,m}$ from the cylindrical coordinate system using the transition formulas (8) are rewritten as \vec{u}_k^{\pm} into Cartesian one.

Six more equations are formed when the boundary conditions on the inner surfaces of the pipes (2) are satisfied. For this purpose, the stress operator is applied to the functions (7), and the expressions for \vec{e}_φ and \vec{e}_z in stresses along \vec{e}_ρ remain in the displacements. These expressions are equated to functions (2), to which the Fourier integral along the axis z and the Fourier series in the angle φ are applied.

Three equations are written for the boundary conditions on the surface of the cavity. For this purpose, the stress operator is applied to functions (6), and the Fourier integral along the axis z and the Fourier series in the angle φ are applied to (3). After that, they are equated to each other. Basic solutions \vec{u}_k^{\pm} from the Cartesian coordinate system using the transition formulas (9) are rewritten as $\vec{R}_{k,m}$ into a cylindrical one.

Another 12 equations are formed when the conjugation conditions between the layer and each pipe (4), (5) are met. When these conditions are met, the basic solutions \vec{u}_k^{\pm} are rewritten from the Cartesian coordinate system through $\vec{R}_{k,m}$ into local cylindrical ones using the transition functions (9). In addition, the formulas for the transition of basic solutions from one local cylindrical coordinate system to another (10) are used.

And the first six equations $H_k(\lambda, \mu)$ and $\tilde{H}_k(\lambda, \mu)$ were derived through $B_{k,m}^{(p)}(\lambda)$ and substituted into other equations. Having freed the left and right sides from series and integrals, we obtained an infinite system

of 21 linear algebraic equations of the second kind, to which the reduction method can be applied. As a result of the solution, the unknowns $B_{k,m}^{(1)}(\lambda)$, $B_{k,m}^{(2)}(\lambda)$, $B_{k,m}^{(3)}(\lambda)$, $A_{k,m}^{(1)}(\lambda)$, $\tilde{A}_{k,m}^{(1)}(\lambda)$, $A_{k,m}^{(2)}(\lambda)$, $\tilde{A}_{k,m}^{(2)}(\lambda)$ were found. Obtained function values $B_{k,m}^{(1)}(\lambda)$ and $B_{k,m}^{(2)}(\lambda)$ were substituted into the expression for $H_k(\lambda, \mu)$ and $\tilde{H}_k(\lambda, \mu)$. Thanks to this, all unknowns of equations (6) and (7) are found.

Numerical studies of the stressed state

The problem is solved numerically for a layer with two cylindrical pipes and a cylindrical cavity under a given cantilever load (Fig. 2).

Geometric parameters of the model: pipes and cylindrical cavity are located on the same horizontal axis ($\alpha_{12}=0$, $\alpha_{13}=\pi$), distance between pipes $L_{12}=40$ mm, distance to cylindrical cavity $L_{13}=40$ mm, outer radius of pipes $R_1=R_2=R_3=15$ mm, internal one $r_1=r_2=10$ mm, distances to the upper and lower boundaries of the layer $h=\tilde{h}=20$ mm.

Physical characteristics of the layer: aluminum alloy D16T, Poisson's ratio $\nu_0=0.3$, modulus of elasticity $E_0=7.1 \times 10^4$ MPa. Physical characteristics of pipes: steel SHKH15, Poisson's ratio $\nu_1=\nu_2=0.28$, modulus of elasticity $E_1=E_2=2.16 \times 10^5$ MPa.

At the upper boundary of the layer, stresses are given in the form of a unit wave $\sigma_y^{(h)}(x, z) = \frac{-10^8}{(z^2 + 10^2)^2 \cdot ((x + c)^2 + 10^2)^2}$, $c=160$ mm and zero tangential stresses $\tau_{yx}^{(h)} = \tau_{yz}^{(h)} = 0$, at the lower boundary of the layer – zero stresses $\sigma_y^{(\tilde{h})}(x, z) = \tau_{yz}^{(\tilde{h})} = \tau_{yx}^{(\tilde{h})} = 0$ are given. Zero normal displacements and tangential stresses are given on the inner surfaces of the pipes $U_0^{(p)}(\varphi_p, z) = \tau_1^{(p)}(\varphi_p, z) = \tau_2^{(p)}(\varphi_p, z) = 0$, $p=1 \dots 2$. Zero stresses are set on the surface of the cavity $\sigma_p^{(3)} = \tau_{p\varphi}^{(3)} = \tau_{pz}^{(3)} = 0$.

The accuracy of meeting the boundary conditions depends on the number of terms in the Fourier series and the order of the system of equations – m . For given geometric parameters, the convergence of boundary conditions is presented in Table 1.

Fig. 2. Cantilever load of a layer on two embedded cylindrical supports with a cylindrical cavity

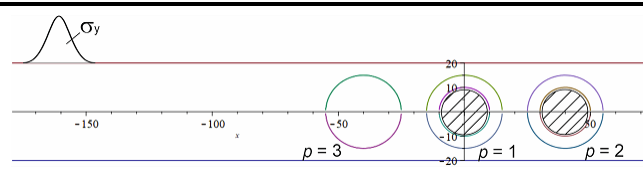


Table 1. Convergence of boundary conditions

Stress	$m=2$	$m=3$	$m=4$	$m=5$	$m=6$
$\sigma_y^{(h)}(x, z)$	-0.98979	-0.996239	-0.999133	-0.99982	-0.999954
$\sigma_y^{(\tilde{h})}(x, z)$	-0.0026	-0.00025	-0.000013	-2×10^{-6}	-1×10^{-6}

The stress state analysis was performed at $m=6$.

Fig. 3 shows the stress σ_φ on the inner and outer surfaces of pipes when $z=0$.

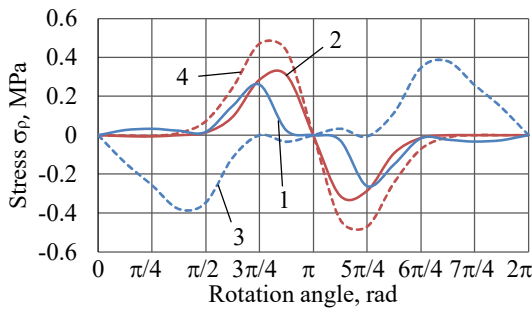
Stresses σ_φ are maximum on the inner surfaces of the pipes (Fig. 3, lines 3, 4) and arise under the influence of the load and zero normal displacements at the supports. The stress σ_φ on the inner surface of the pipe $p=2$ (Fig. 3, line 4) is opposite in sign and slightly greater than the stress σ_φ on the pipe $p=1$ (Fig. 3, line 3). These stresses also have a different sign depending on the part of the pipe where they are considered (upper or lower). The stresses σ_φ on the inner surfaces of the pipes are also greater on the pipe $p=2$ (Fig. 3, line 2).

The outer surfaces of the pipes are rigidly connected to the layer, therefore the stress σ_φ on the conjugation surface in the body of the layer is equal to the stress σ_φ in the pipe body, i.e. on the surfaces of the cavities $p=1$ and $p=2$ in the body of the layer, the stresses indicated in Fig. 3 (lines 1, 2) arise.

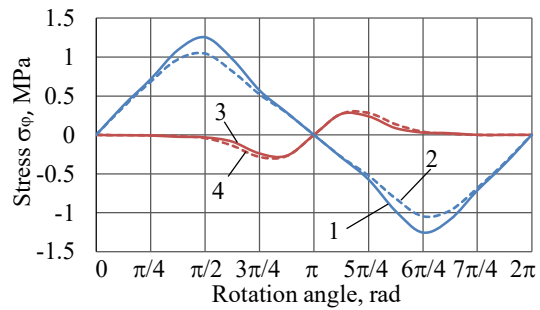
The stresses σ_φ on the outer and inner surfaces of the pipes at $z=0$ are shown in Fig. 4.

The stresses σ_φ in the pipe body $p=1$ (Fig. 4, lines 1, 2) are maximum on the outer surface of the pipe, significantly exceed the stresses σ_φ in the pipe body $p=2$ and the given unit stresses σ_y .

The stresses σ_φ in the pipe body $p=2$ (Fig. 4, lines 3, 4) on the outer and inner surfaces of the pipe are almost the same and are significantly less than the stresses in the pipe body $p=1$.

**Fig. 3. Stresses σ_ρ on pipe surfaces:**

1 – pipe $p=1$, $\rho=R_1$; 2 – pipe $p=1$, $\rho=r_1$;
3 – pipe $p=2$, $\rho=R_2$; 4 – pipe $p=2$, $\rho=r_2$

**Fig. 4. Stresses σ_ϕ on pipe surfaces:**

1 – pipe $p=1$, $\rho=R_1$; 2 – pipe $p=1$, $\rho=r_1$;
3 – pipe $p=2$, $\rho=R_2$; 4 – pipe $p=2$, $\rho=r_2$

The stresses σ_ϕ on the surfaces of cylindrical holes in the layer body, including at the point of contact with the pipes, at $z=0$, are shown in Fig. 5.

The maximum stress values $\sigma_\phi = \pm 1.7$ MPa are observed on the surface of the cylindrical cavity $p=3$, in its upper part (Fig. 5, line 3). This significantly exceeds the specified unit stresses σ_y . The maximum stress σ_ϕ values on the conjugation surface $p=1$ in the layer body (line 1) is $\sigma_\phi = \pm 0.4104$ MPa, on the conjugation surface $p=2$ in the layer body it is equal to zero. A significant reduction in stresses on the cavities $p=1$ and $p=2$ is ensured, in particular, by steel sleeves.

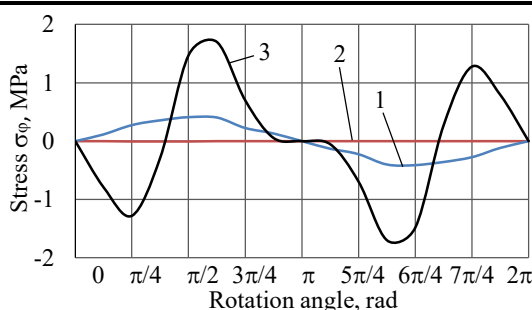
The tangential stresses $\tau_{\rho\phi}$ on the surfaces of the cylindrical holes of the layer at the point of contact with the pipes (in the layer body), at $z=0$ are shown in Fig. 6.

Under the conditions of rigid connection of pipes with a layer, the tangential stresses $\tau_{\rho\phi}$ on the conjugation surface in the pipe body are equal to the stresses $\tau_{\rho\phi}$ in the layer body (Fig. 6). The tangential stresses $\tau_{\rho\phi}$ at the point of the layer conjugation with the pipe $p=2$ are concentrated in the left part of the connection (Fig. 6, line 2).

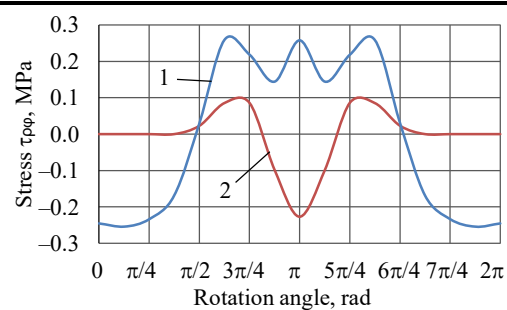
The tangential stresses $\tau_{\rho\phi}$ at the point of the layer conjugation with the pipe $p=1$ (Fig. 6, line 1) are greater than the stresses $\tau_{\rho\phi}$ at the point of the layer conjugation with the pipe $p=2$.

The stresses σ_x on the upper and lower surfaces of the layer along the x axis at $z=0$ are shown in Fig. 7.

The stresses σ_x along the x -axis at the upper boundary of the layer are maximum $\sigma_x = \pm 1.9648$ MPa at a distance of $x = -30$ mm, i.e. above the cavity ($p=3$), and significantly exceed the specified unit stresses σ_y . At a distance of $x = -160$ mm (at the location of the specified unit stress σ_y), the stresses σ_x at the upper boundary also have an extremum $\sigma_x = -0.9596$ MPa.

**Fig. 5. Stresses σ_ϕ on the surfaces of the cylindrical holes of the layer:**

1 – at the point of contact with the pipe ($p=1$);
2 – at the point of contact with the pipe ($p=2$);
3 – on the surface of the cavity ($p=3$)

**Fig. 6. Tangential stresses $\tau_{\rho\phi}$ at the points of the layer conjugation with the pipes:**

1 – support $p=1$; 2 – support $p=2$

Conclusions

An analytical-numerical approach to solving a mixed problem of the theory of elasticity for a layer with two longitudinal cylindrical pipes and a cylindrical cavity is proposed for the case when stresses are given on the upper and lower boundaries of the layer, on the inner surfaces of the pipes - conditions of smooth contact, and on the cavity - stresses.

For the first time, a solution for a layer with two cylindrical pipes and a cylindrical cavity is written in analytical form.

The problem is reduced to an infinite system of linear algebraic equations, which allows the application of the reduction method to it. The application of the analytical-numerical generalized Fourier method allowed obtaining a solution to the problem with a given accuracy.

The numerical analysis of the stress state of the layer and thick-walled pipes under a given cantilever load showed that:

– stresses σ_ϕ and σ_x in the conjugation $p=1$ on the surface of the cavity $p=3$ and on the flat surfaces of the layer significantly exceed the specified unit σ_y ;

– when comparing the stresses in the places of cylindrical supports, the stresses σ_ϕ and $\tau_{\phi\phi}$ in absolute values are greater on the surfaces of the pipe $p=1$, and the stress σ_ρ is greater on the surfaces of the pipe $p=2$.

The proposed solution method allows to obtain the results of the stress-strain state of cantilever elements of aircraft structures, to evaluate the influence of the material and geometric parameters on the magnitude of the stress distribution in other structures of machines and mechanisms, which can be represented in the form of models similar to the one under consideration.

In the future, to develop the specified research topic, it is necessary to consider models with other boundary conditions. One of such options is to take into account smooth contacts between the layer and pipes.

References

1. Tekkaya, A. E. & Soyarslan, C. (2014). Finite element method. In: Laperrière, L., Reinhart, G. (eds) CIRP Encyclopedia of Production Engineering. Berlin, Heidelberg: Springer, pp. 508–514. https://doi.org/10.1007/978-3-642-20617-7_16699.
2. Ansys. (n.d.). *Static structural simulation using Ansys Discovery*. Ansys Courses. Retrieved February 27, 2025, from <https://courses.ansys.com/index.php/courses/structural-simulation>.
3. Revo, S. L., Avramenko, T. H., Melnychenko, M. M., & Ivanenko, K. O. (2021). *Fizyko-mekhanichni kharakterystyky nanokompozitsiynykh materialiv na osnovi storoplastu* [Physico-mechanical characteristics of nanocomposite materials based on fluoroplastic]. *Visnyk Kyivskoho natsionalnoho universytetu imeni Tarasa Shevchenka. Seriia fizyko-matematichni nauky – Bulletin of Taras Shevchenko National University of Kyiv Series Physics & Mathematics*, no. 3, pp. 107–110 (in Ukrainian). <https://doi.org/10.17721/1812-5409.2021/3.20>.
4. Kondratiev, A. V., Gaidachuk, V. E., & Kharchenko, M. E. (2019). Relationships between the ultimate strengths of polymer composites in static bending, compression, and tension. *Mechanics of Composite Materials*, vol. 55, iss. 2, pp. 259–266. <https://doi.org/10.1007/s11029-019-09808-x>.
5. Guz, A. N., Kubenko, V. D., & Cherevko, M. A. (1978). *Difraktsiya uprugikh voln* [Elastic wave diffraction]. Kyiv: Naukova dumka, 307 p. (in Russian).
6. Grinchenko, V. T. & Meleshko, V. V. (1981). *Garmonicheskiye kolebaniya i volny v uprugikh telakh* [Harmonic vibrations and waves in elastic bodies]. Kyiv: Naukova dumka, 284 p. (in Russian).
7. Fesenko, A. & Vaysfel'd, N. (2019). The wave field of a layer with a cylindrical cavity. In: Gdoutos, E. (eds) *Proceedings of the Second International Conference on Theoretical, Applied and Experimental Mechanics. ICTAEM 2019. Structural Integrity*, vol. 8. Cham: Springer, pp. 277–282. https://doi.org/10.1007/978-3-030-21894-2_51.
8. Fesenko, A. & Vaysfel'd, N. (2021). The dynamical problem for the infinite elastic layer with a cylindrical cavity. *Procedia Structural Integrity*, vol. 33, pp. 509–527. <https://doi.org/10.1016/j.prostr.2021.10.058>.
9. Malits, P. (2021). Torsion of an elastic half-space with a cylindrical cavity by a punch. *European Journal of Mechanics – A/Solids*, vol. 89, article 104308. <https://doi.org/10.1016/j.euromechsol.2021.104308>.

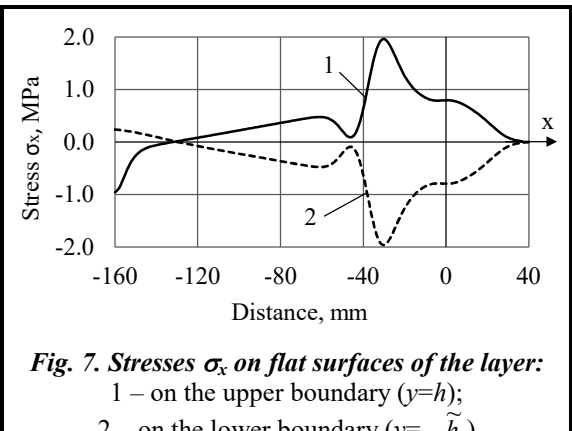


Fig. 7. Stresses σ_x on flat surfaces of the layer:

1 – on the upper boundary ($y=h$);

2 – on the lower boundary ($y=-h$)

10. Jafari, M., Chaleshtari, M. H. B., Khoramishad, H., & Altenbach H. (2022). Minimization of thermal stress in perforated composite plate using metaheuristic algorithms WOA, SCA and GA. *Composite Structures*, vol. 304, part 2, article 116403. <https://doi.org/10.1016/j.comstruct.2022.116403>.
11. Nikolayev, A. G. & Protsenko, V. S. (2011). *Obobshchennyj metod Fureye v prostranstvennykh zadachakh teorii uprugosti* [Generalized Fourier method in spatial problems of the theory of elasticity]. Kharkiv: National Aerospace University "Kharkiv Aviation Institute", 344 p. (in Russian).
12. Nikolaev, A. G. & Tanchik, E. A. (2015). The first boundary-value problem of the elasticity theory for a cylinder with N cylindrical cavities. *Numerical Analysis and Applications*, vol. 8, pp. 148–158. <https://doi.org/10.1134/S1995423915020068>.
13. Nikolaev, A. G. & Tanchik, E. A. (2016). Stresses in an elastic cylinder with cylindrical cavities forming a hexagonal structure. *Journal of Applied Mechanics and Technical Physics*, vol. 57, pp. 1141–1149. <https://doi.org/10.1134/S0021894416060237>.
14. Nikolaev, A. G. & Tanchik, E. A. (2016). Model of the stress state of a unidirectional composite with cylindrical fibers forming a tetragonal structure. *Mechanics of Composite Materials*, vol. 52, pp. 177–188. <https://doi.org/10.1007/s11029-016-9571-6>.
15. Ukrayinets, N., Murahovska, O., & Prokhorova, O. (2021). Solving a one mixed problem in elasticity theory for half-space with a cylindrical cavity by the generalized Fourier method. *Eastern-European Journal of Enterprise Technologies*, vol. 2, no. 7 (110), pp. 48–57. <https://doi.org/10.15587/1729-4061.2021.229428>.
16. Miroshnikov, V., Denysova, T., & Protsenko, V. (2019). *Doslidzhennia pershoi osnovnoi zadachi teorii pruzhnosti dlja sharu z tsylindrychnoi porozhnynoi* [The study of the first main problem of the theory of elasticity for a layer with a cylindrical cavity]. *Opir materialiv i teoriia sporud – Strength of Materials and Theory of Structures*, no. 103, pp. 208–218 (in Ukrainian). <https://doi.org/10.32347/2410-2547.2019.103.208-218>.
17. Miroshnikov, V. Yu., Medvedeva, A. V., & Oleshkevich, S. V. (2019). Determination of the stress state of the layer with a cylindrical elastic inclusion. *Materials Science Forum*, vol. 968, pp. 413–420. <https://doi.org/10.4028/www.scientific.net/msf.968.413>.
18. Miroshnikov, V. Yu. (2019). Investigation of the stress state of a composite in the form of a layer and a half space with a longitudinal cylindrical cavity at stresses given on boundary surfaces. *Journal of Mechanical Engineering – Problemy Mashynobuduvannia*, vol. 22, no. 4, pp. 24–31. <https://doi.org/10.15407/pmach2019.04.024>.
19. Miroshnikov, V. Yu., Savin, O. B., Hrebennikov, M. M., & Demenko, V. F. (2023). Analysis of the stress state for a layer with two incut cylindrical supports. *Journal of Mechanical Engineering – Problemy Mashynobuduvannia*. 2023. Vol. 26. No. 1. P. 15–22. <https://doi.org/10.15407/pmach2023.01.015>.
20. Miroshnikov, V. (2023). Rotation of the layer with the cylindrical pipe around the rigid cylinder. In: Altenbach H., et al. *Advances in Mechanical and Power Engineering. CAMPE 2021. Lecture Notes in Mechanical Engineering*. Cham: Springer, pp. 314–322. https://doi.org/10.1007/978-3-031-18487-1_32.
21. Kosenko, M. (2024). *Rozviazok zadachi teorii pruzhnosti dlja sharu z tsylindrychnymy vrizanymy oporamy u vyhliadi porozhnyny ta truby: zhorstke zakriplennia* [Solution of the problem of the theory of elasticity for a layer with cylindrical embedded supports in the form of a cavity and a pipe: rigid fastening]. *Modern problems of development of the aerospace industry of Ukraine: engineering, business, law: abstracts of the interdisciplinary scientific and practical conference (November 5, 2024, Kharkiv, Ukraine)*. Kharkiv: National Aerospace University "Kharkiv Aviation Institute", pp. 170–174 (in Ukrainian).
22. Miroshnikov, V. Yu., Savin, O. B., Kosenko, M. L., & Ilin, O. O. (2024). *Analiz napruzenoho stanu sharu z dvoma tsylindrychnymy vrizanymy oporamy ta tsylindrychnymy vtulkamy* [Analysis of the stress state of a layer with two cylindrical embedded supports and cylindrical bushings]. *Vidkryti informatsiini ta kompiuterni intekhnolohii – Open Information and Computer Integrated Technologies*, no. 101, pp. 112–126 (in Ukrainian). <https://doi.org/10.32620/oikit.2024.101.08>.

Received 07 September 2025

Accepted 14 October 2025

Аналіз напруженено-деформованого стану шару з циліндричною порожниною і врізаними опорами з втулками**М. Л. Косенко**

Національний аерокосмічний університет «Харківський авіаційний інститут»,
61070, Україна, м. Харків, вул. Вадима Манька, 17

В авіакосмічній галузі й машинобудуванні поширеним є застосування циліндричних врізаних опор для деталей. Для розрахунку подібних з'єднань використовують спрощення або наближення. У статті запропоновано методику розрахунку шару на двох поздовжньо врізаних циліндричних опорах. Між опорами й шаром розташовані втулки (тovстостінні труби), шар послаблений поздовжньою циліндричною порожнинною. На нижній і верхній поверхнях шару задані напруження, а на внутрішніх поверхнях труб – умови гладкого контакту, на поверхні порожнини – напруження. Для розв'язання задачі використано рівняння Ламе, де для шару застосовано декартову систему координат, а для труб і циліндричної порожнини – локальні циліндричні системи. Поєднання базисних розв'язків у різних системах координат здійснюється за допомогою узагальненого методу Фур'є. Виходячи з граничних умов й умов спряження, отримано нескінченну систему інтегро-алгебраїчних рівнянь, яка зводиться до лінійних алгебраїчних рівнянь другого роду й розв'язується за допомогою методу редукції. Напруженено-деформований стан у кожній точці пружин з'єднаних тіл визначено також із рівняння Ламе з використанням узагальненого методу Фур'є до базисних розв'язків. Показано, що точність результацій у цьому випадку залежить від наближення граничних поверхонь одна до одної та від порядку системи рівнянь. Чисельні дослідження проведено для шару з опорами й порожнинною, розташованими на одній прямій, при дії консольного навантаження. Аналіз напруженого стану отримано в зонах циліндричних отворів шару й в тілі втулок. Максимальні напруження перевищують задані і виникають у місці розташування циліндричної порожнини. Запропонований метод розв'язання дає можливість отримувати результації напруженено-деформованого стану консольних елементів конструкцій літаків, оцінювати вплив матеріалу й геометричних параметрів на величини розподілення напруженень в інших конструкціях машин і механізмів, які можуть бути представлені у вигляді моделей, подібних розглянутій.

Ключові слова узагальнений метод Фур'є, рівняння Ламе, шар з циліндричними включеннями, нескінченна система інтегро-алгебраїчних рівнянь, циліндрична порожнina.

Література

1. Tekkaya A. E., Soyarslan C. Finite element method. In: Laperrière L., Reinhart G. (eds) CIRP Encyclopedia of Production Engineering. Berlin, Heidelberg: Springer, 2014. P. 508–514. https://doi.org/10.1007/978-3-642-20617-7_16699.
2. Static Structural Simulation Using Ansys Discovery. <https://courses.ansys.com/index.php/courses/structural-simulation>.
3. Рево С. Л., Авраменко Т. Г., Мельниченко М. М., Іваненко К. О. Фізико-механічні характеристики нанокомпозіційних матеріалів на основі фторопласти. *Вісник Київського національного університету імені Тараса Шевченка. Серія фізико-математичні науки*. 2021. № 3. С. 107–110. <https://doi.org/10.17721/1812-5409.2021/3.20>.
4. Kondratiev A. V., Gaidachuk V. E., Kharchenko M. E. Relationships between the ultimate strengths of polymer composites in static bending, compression, and tension. *Mechanics of Composite Materials*. 2019. Vol. 55. Iss. 2, P. 259–266. <https://doi.org/10.1007/s11029-019-09808-x>.
5. Гузь А. Н., Кубенко В. Д., Черевко М. А. Дифракція упругих волн. Київ: Наукова думка, 1978. 307 с.
6. Гринченко В. Т., Мелешко В. В. Гармонические колебания и волны в упругих телах. Київ: Наукова думка, 1981. 284 с.
7. Fesenko A., Vaysfel'd N. The wave field of a layer with a cylindrical cavity. In: Gdoutos, E. (eds) *Proceedings of the Second International Conference on Theoretical, Applied and Experimental Mechanics. ICTAEM 2019. Structural Integrity*. Cham: Springer, 2019. Vol. 8. P. 277–282. https://doi.org/10.1007/978-3-030-21894-2_51.
8. Fesenko A., Vaysfel'd N. The dynamical problem for the infinite elastic layer with a cylindrical cavity. *Procedia Structural Integrity*. 2021. Vol. 33. P. 509–527. <https://doi.org/10.1016/j.prostr.2021.10.058>.
9. Malits P. Torsion of an elastic half-space with a cylindrical cavity by a punch. *European Journal of Mechanics – A/Solids*. 2021. Vol. 89. Article 104308. <https://doi.org/10.1016/j.euromechsol.2021.104308>.
10. Jafari M., Chaleshtari M. H. B., Khoramishad H., Altenbach H. Minimization of thermal stress in perforated composite plate using metaheuristic algorithms WOA, SCA and GA. *Composite Structures*. 2022. Vol. 304. Part 2. Article 116403. <https://doi.org/10.1016/j.compstruct.2022.116403>.

11. Николаев А. Г., Проценко В. С. Обобщенный метод Фурье в пространственных задачах теории упругости. Харьков: Нац. аэрокосм. ун-т им. Н. Е. Жуковского «ХАИ», 2011. 344 с.
12. Nikolaev A. G., Tanchik E. A. The first boundary-value problem of the elasticity theory for a cylinder with N cylindrical cavities. *Numerical Analysis and Applications*. 2015. Vol. 8. P. 148–158. <https://doi.org/10.1134/S1995423915020068>.
13. Nikolaev A. G., Tanchik E. A. Stresses in an elastic cylinder with cylindrical cavities forming a hexagonal structure. *Journal of Applied Mechanics and Technical Physics*. 2016. Vol. 57. P. 1141–1149. <https://doi.org/10.1134/S0021894416060237>.
14. Nikolaev A. G., Tanchik E. A. Model of the stress state of a unidirectional composite with cylindrical fibers forming a tetragonal structure. *Mechanics of Composite Materials*. 2016. Vol. 52. P. 177–188. <https://doi.org/10.1007/s11029-016-9571-6>.
15. Ukrayinets N., Murahovska O., Prokhorova O. Solving a one mixed problem in elasticity theory for half-space with a cylindrical cavity by the generalized Fourier method. *Eastern-European Journal of Enterprise Technologies*. 2021. Vol. 2. No. 7 (110). P. 48–57. <https://doi.org/10.15587/1729-4061.2021.229428>.
16. Мірошніков В. Ю., Денисова Т. В., Проценко В. С. Дослідження першої основної задачі теорії пружності для шару з циліндричною порожниною. *Опір матеріалів і теорія споруд*. 2019. № 103. С. 208–218. <https://doi.org/10.32347/2410-2547.2019.103.208-218>.
17. Miroshnikov V. Yu., Medvedeva A. V., Oleshkevich S. V. Determination of the stress state of the layer with a cylindrical elastic inclusion. *Materials Science Forum*. 2019. Vol. 968. P. 413–420. <https://doi.org/10.4028/www.scientific.net/msf.968.413>.
18. Miroshnikov V. Yu. Investigation of the stress state of a composite in the form of a layer and a half space with a longitudinal cylindrical cavity at stresses given on boundary surfaces. *Journal of Mechanical Engineering – Problemy Mashynobuduvannia*. 2019. Vol. 22. No. 4. P. 24–31. <https://doi.org/10.15407/pmach2019.04.024>.
19. Miroshnikov V. Yu., Savin O. B., Hrebennikov M. M., Demenko V. F. Analysis of the stress state for a layer with two in-cut cylindrical supports. *Journal of Mechanical Engineering – Problemy Mashynobuduvannia*. 2023. Vol. 26. No. 1. P. 15–22. <https://doi.org/10.15407/pmach2023.01.015>.
20. Miroshnikov V. Rotation of the layer with the cylindrical pipe around the rigid cylinder. In: Altenbach H., et al. *Advances in Mechanical and Power Engineering. CAMPE 2021. Lecture Notes in Mechanical Engineering*. Cham: Springer, 2023. P. 314–322. https://doi.org/10.1007/978-3-031-18487-1_32.
21. Косенко М. Розв'язок задачі теорії пружності для шару з циліндричними врізаними опорами у вигляді порожнини та труби: жорстке закріплення. *Сучасні проблеми розвитку аерокосмічної галузі України: інженерія, бізнес, право: тези міждисциплінарної науково-практичної конференції* (5 листопада 2024, м. Харків, Україна). Харків: Нац. аерокосм. ун-т «ХАІ», 2024. С. 170–174.
22. Мірошніков В. Ю., Савін О. Б., Косенко М. Л., Ільїн О. О. Аналіз напруженого стану шару з двома циліндричними врізаними опорами та циліндричними втулками. *Відкриті інформаційні та комп'ютерні інтегровані технології*. 2024. № 101. С. 112–126. <https://doi.org/10.32620/oikit.2024.101.08>.